
Nuclear Translocation of Apoptosis Inducing Factor and Subsequent DNA Fragmentation by Reactive Oxygen Species After Permanent Focal Cerebral Ischemia in Mice

Department of Neurology and Microbiology¹, Yonsei University College of Medicine, Brain Research Institute

Yang-Je Cho, M.D., Yong Hyun Lee, M.S., Kyoung-Joo Cho, M.S., Doo Jae Lee, Ph.D., Hyun-Woo Kim, B.S., Hyun-Jung Kim, B.S., Byung In Lee, M.D., Sang-Nae Cho, Ph.D.¹, and Gyung Whan Kim, M.D., Ph.D.

Background: Recently, the mitochondrial proapoptotic protein, apoptosis-inducing factor (AIF), and its nuclear translocation have been reported in caspase-independent neuronal apoptosis. However, it is not elucidated whether oxidative signaling is involved in the nuclear translocation of AIF and subsequent caspase-independent apoptotic cell death. We investigated whether oxidative signaling induces nuclear translocation of AIF and subsequent caspase-independent apoptosis-associated DNA fragmentation after permanent focal cerebral ischemia (FCI). **Methods:** Adult male ICR mice were subjected to permanent FCI by intraluminal suture blockade of middle cerebral artery. Immunohistochemistry and Western blot analysis were performed. Large-scale DNA fragmentation was evaluated by pulse field gel electrophoresis and apoptotic cell death was quantified. Manganese tetrakis (4-benzoic acid) porphyrin (MnTBAP), which mimics mitochondrial superoxide dismutase, was used to determine whether the production of reactive oxygen species is required for the induction in AIF translocation. **Results:** Western blot analysis showed that the nuclear translocation of AIF occurred as early as 2 hours after permanent FCI. Immunostaining for AIF also confirmed early nuclear translocation of AIF after permanent FCI. Large-scale DNA fragmentation was detected 8 hours after permanent FCI. MnTBAP-treatment attenuated AIF translocation and blocked large-scale DNA fragmentation. Caspase-3 activity was similarly inhibited between the pan-caspase inhibitor- and MnTBAP-treated mice, but the amount of apoptosis-associated DNA fragmentation in the MnTBAP-treated mice was less than in the pan-caspase inhibitor-treated mice ($P < 0.001$). In addition, infarction volume was also decreased by MnTBAP. **Conclusions:** These results suggest that reactive oxygen species induce the caspase-independent nuclear translocation of AIF and subsequent apoptosis-associated DNA fragmentation after permanent FCI.

(*Korean Journal of Stroke* 2005;7(2): 214~223)

Key Words: Apoptosis, Ischemic brain injury, Oxidative stress, Apoptosis-inducing factor

.....
:
134

(reactive oxygen species)

TEL : 82-2-2228-1600
FAX : 82-2-393-0705
E-mail : gyungkim@yumc.yonsei.ac.kr

가 ,

[1]. (superoxide anion) (apoptosis) (cell death) (apoptosis)가 , 가 ATP (e.g. ischemic penumbra) (death-receptor pathway) DNA (fragmentation) [5].

[6], 가 cytochrome c SMAC (second mitochondria-derived activator of caspase)/DIABLO (direct inhibitor-of-apoptosis protein binding protein with low pI), (apoptosis-inducing factor, AIF), endonuclease G [7]. caspase caspase-activated DNase (CAD)가 DNA caspase [6,8]. caspase

[9,10], AIF가 caspase (key initiator) [11]. AIF (effector) (chromatin) (~ 50 kbp) DNA [6, 8]. AIF (translocate) , caspase [6,12], caspase AIF [6,12-15]. AIF [16,17] [11] [18], [19] AIF AIF 가 (superoxide scavenger) manganese tetrakis(4-Benzoic acid) porphyrin chloride (MnTBAP) [20] AIF가 AIF

caspase DNA .

1. Association for Assessment and Accreditation of Laboratory Animal Care (AAALAC) . ICR (3 , 35-40 g)(Daehan Biolink Co., Chunbuk, South Korea) (middle cerebral artery occlusion, MCAO) [3,21,22]. 20% isoflurane (70%/30%) heating pad lamp 37 ±0.5 가 (Roche Diagnostics, Basel, Switzerland). 11.0 mm (Ethicon, Edinburg, UK) 6-0 . MnTBAP (Biomol International, Plymouth Meeting, PA, USA) vehicle() 30

2. 1, 2, 4, 24 {120 mM HEPES-KOH pH 7.05, 10 mM NaCl, 1.5 mM MgCl₂, 1 mM Na-EDTA, 1 mM Na-EGTA, 1 mM DTT, 0.1 mM PMSF, proteinase inhibitor cocktail (Sigma, St Louis, MO, USA), 250 mM sucrose}

750xg	4	10
4	15	4
15	1,025xg	
4	15	
4	20	16,000xg
4	15	10,000xg
		3% Ficoll (120 mM mannitol, 30 mM sucrose, 25 M EDTA)
		, 6% Ficoll (240 mM mannitol, 60 mM sucrose, 50 M EDTA)
4	25	16,000xg

[18,19,24].
Bradford protein assay (Bio-Rad,
Hercules, CA, USA)

3. Western blot analysis

6% polyacrylamide gel
, polyvinylidene fluoride (PVDF)
, 16 3% skim milk (10 mmol/L Tris,
pH 8.0, 150 mmol/L NaCl, 0.1% Tween-20)
blocking 1:200
goat anti-AIF polyclonal antibody (Santa Cruz
Biotechnology, Santa Cruz, CA, USA)
1 , 3% skim milk 2
blocking horseradish peroxidase-
linked anti-goat IgG , ECL plus kit
(Amersham International, Buckinghamshire,
England) Image
analyzer LAS-1000 plus (Fuji Film Co., Tokyo,
Japan) TINA 2.0 (Raytest Isotopen-
messgerate GmbH, Straubenhardt, Germany)
[18,19,24].

4.

Urethane 10 U/mL 가
3.7%
, 3.7%
, vibratome 50 μm
[26].
peroxidase phosphate-buffered saline (PBS,
pH 7.4) 0.3% Triton X-100 0.65% NaN₃, 1%
H₂O₂ 30
60 20% rabbit serum
, 1:200 anti-AIF 4
16 . Vectastatin Elite ABC Kit
(Vector Laboratories, Burlingame, CA, USA)
diaminobenzidine
(DAB; Sigma) , methyl green
AIF neuron-spe
cific nuclear protein (NeuN; Chemicon,
Temecula, CA, USA) goat polyclonal anti-AIF
. NeuN
kit (DAKO ARK kit; Dako,
Carpinteria, CA, USA)
. AIF
AIF
avidin fluorescent avidin DCS (50 μg
/mL; Vector Laboratories) Cy™ 3가

1:200 anti-goat IgG (Jackson ImmunoResearch,
West Grove, PA, USA) 1
LSM510 confocal laser
scanning (Carl Zeiss, Thornwood, NY,
USA)

5. in situ

4 oxidized hydroethidine (HEt)
[2,21,22,26]. HEt (Molecular Probes)
dimethylsulfoxide (DMSO) 100 mg/mL
PBS 1:100
ICR 1 200 μl HEt
10 U/mL 가
3.7%
. 3.7% formaldehyde 16 4
vibratome 50 μm
Hoechst 33258 (Molecular Probes)
. Oxidized Het com-
puterized digital camera system (Ex =
510-550 nm, Em>580 nm; BX51, Olympus,
Tokyo, Japan)
(MetaMorpho imaging, version 5.0;
Molecular devices, Downington, PA, USA)[3,26].

6. Pulse Field Gel Electrophoresis

AIF DNA (large-
scale DNA fragmentation)
Pulse Field Gel Electrophoresis (PFGE)
. Chromosomal DNA
agarose plug CHEF Mammalian
Genomic DNA Plug kit (Bio-Rad Hercules, CA,
USA) PFGE [25]. Kit
(15~20 mg) 50
2% low melting point (LMP) agarose
agarose plug . plug 50
, 1 mg/mL proteinase K 16
. DNA agarose plug
well LMP agarose
. PFGE CHEF-DR III Pulse Field
Electrophoresis Systems (Bio-Rad)
. DNA 1.2% agarose gel 14
17 . 180
V, 120 V

0.1 ~ 10 Gel ethidium bromide
(EtBr) UV

7. MnTBAP

50 $\mu\text{g}/\mu\text{l}$ MnTBAP
MCAO 30 (2 μl , medio-
lateral = 1.0 mm; anteroposterior = 0.2 mm;
dorsoventral = 3.1 mm). MnTBAP
vehicle

8. Caspase-3

Caspase-3 caspase-3
N-acetyl-Asp-Glu-Val-Asp-AFC
(DEVD-AFC)
ELISA (Oncogene, San Diego,
CA, USA) Western blot
20 μg
kit caspase buffer E (20 mM HEPES,
pH 7.4, 50 mM NaCl, 0.2 mM EDTA, and 4 mM
dithiothreitol) 37 45
luminescence spectrometer
SL50B (Perkin Elmer, Wellesley, MA, USA)(exci-
tation/emission: 400/505 nm for AFC)

9. Caspase inhibitor

Pan-caspase inhibitor N-Benzoyloxycarbonyl
-val-ala-asp-(O-methyl)-fluoromethyl ketone (z-
VAD.fmk; Sigma) 5 μl Hamilton syringe
(Hamilton, Reno, NV, USA) (2 μl ,
mediolateral = 1.0 mm; anteroposterior = 0.2
mm; dorsoventral = 3.1 mm) MCAO 30
z-VAD.fmk (125 $\mu\text{g}/\mu\text{l}$)
0.3% DMSO vehicle
0.3% DMSO [23].

10. AIF DNA

AIF
, DNA fluorescent
isothiocyanate (FITC)가 1:200 anti-goat
IgG (Jackson Immunoresearch) 1
. PBS 50 μl terminal
deoxynucleotidyl transferase-mediated uridine
5'-triphosphate biotin nick-end labeling
(TUNEL) (terminal deoxynucleotidyl

transferase and fluorecein-dUTP; Roche
Diagnostics, Indianapolis, IN, USA) 37
60 . Vectashield
(Vector Laboratories) LSM510
confocal laser scanning (Carl Zeiss)

11.

DNA
histone DNA
ELISA (Cell death detection kit, Roche
Diagnostics)
oligo-DNA [23].

, 5 가
(50 mM KH₂PO₄, 0.1 mM EDTA, pH
7.8) Teflon homogenizer 750 \times g
10
10,000 \times g 20 spin 100,000 \times g
4 60

kit
ELISA
12.

Vehicle() MnTBAP
, 15 MCAO
, 24
brain matrix
2 mm
2% 2,3,5-triphenyltetra-
zolium chloride (TTC) 가 37 15
1200
dpi , MetaMorpho imaging (version
5.0; Molecular devices)
[22,24].

13.

mean \pm SD
ANOVA
t-test (StatView; SAS
Institute Inc, Cary, NC, USA), p<0.05, p<0.001

1. FCI, MntTBAP, ICR (Table 1).

2. Western blot AIF MCAO 1 ~67kDa (Fig. 1A). AIF 4 24 가 (optical density(OD): Ctr, 0.8 ± 0.2 ; 1 h, 8.0 ± 0.37 ; 2 h, 11.87 ± 0.38 ; 4 h, 14.75 ± 0.4 , 24 h, 28.87 ± 0.79 ; ANOVA, $p < 0.001$)(Fig. 1A).

가 (OD: Ctr, 25 ± 0.95 ; 1 h, 20.25 ± 1.25 ; 2 h, 17.25 ± 0.95 ; 4 h, 14.50 ± 1.29 ; 24 h, 31.25 ± 2.67 ; ANOVA, $p < 0.001$)(Fig. 1A).

3. AIF AIF AIF (Fig. 1B). AIF NeuN 가 (Fig. 1C₁₋₃), AIF NeuN (Fig. 1C₄₋₆).

4. MntTBAP oxidized HET가 (Fig. 2A, arrow heads), 4 vehicle

HEt가 가 (Fig. 2B), MntTBAP (Fig. 2D) HEt (Fig. 2C) 가 MntTBAP vehicle (OD: vehicle, 0.68 ± 0.03 ; MntTBAP, 0.33 ± 0.05 ; unpaired t-test, $P < 0.001$).

5. MntTBAP AIF vehicle 4, MntTBAP (Fig. 3A) Western blot AIF MntTBAP vehicle (OD: vehicle, 11.92 ± 0.94 ; MntTBAP, 2.60 ± 0.27 ; unpaired t-test, $P < 0.001$)(Fig. 3A). AIF MntTBAP 가 AIF MntTBAP vehicle 가 (data not shown). 4 AIF vehicle, MntTBAP AIF (Fig. 3B).

6. MntTBAP DNA 8 ~50kbp DNA PFGE 가, 14 (Fig. 4A), DNA MntTBAP vehicle (Fig. 4B).

7. Caspase AIF Western blot vehicle caspase z-VAD.fmk AIF (OD: vehicle, 11.62 ± 0.69 ; z-VAD.fmk, 11.16 ± 0.82 , NS) (Fig. 5A). 24 AIF TUNEL (Fig. 5Ba), TUNEL AIF (Fig. 5Ba3, arrow heads). Vehicle, z-VAD.fmk, MntTBAP 가 caspase-3, z-VAD.fmk MntTBAP vehicle caspase-

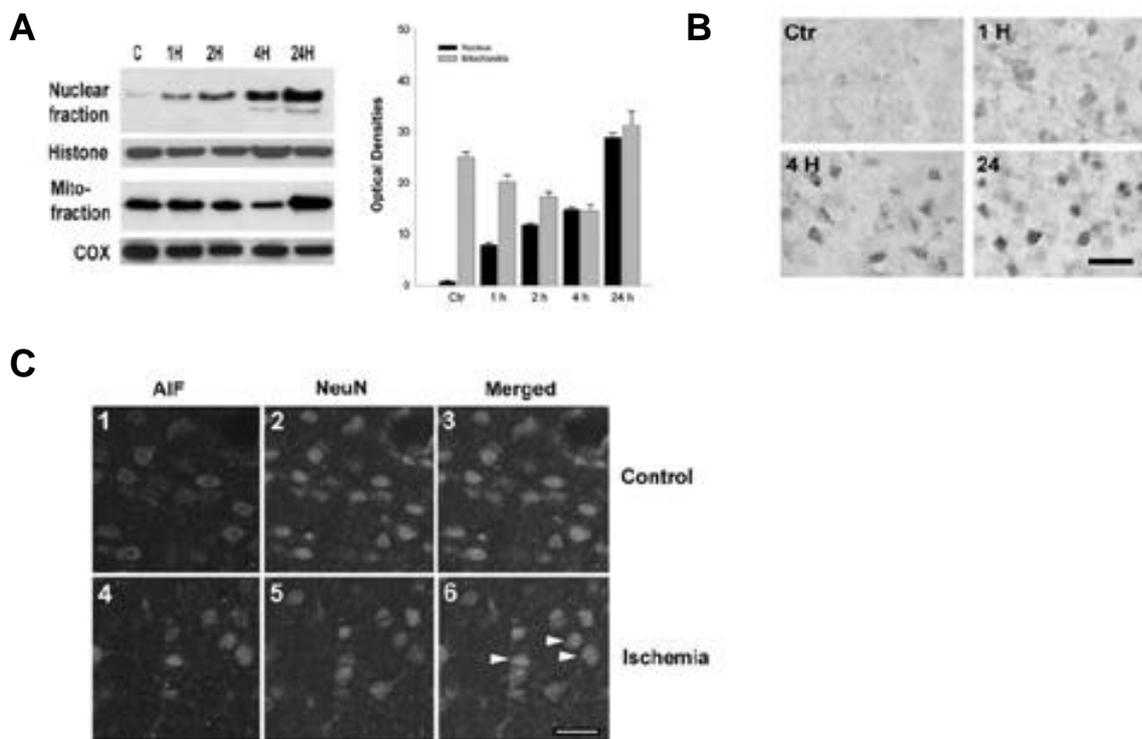


Figure 1. Western blot analysis, immunohistochemical staining, and double labeling immunofluorescence with AIF and NeuN after permanent FCI. (A) Western blot analysis of AIF confirmed successful separation of nuclear and mitochondrial fractions and early nuclear translocation of AIF. Histone and COX were used as the internal controls in the nuclear and mitochondrial fractions each. (B) Immunohistochemistry revealed a time-dependent increase of AIF nuclear translocation. Scale bar = 50 μm . (C) Double labeling immunofluorescence with AIF and NeuN at 4 hours after permanent FCI. AIF (C1), NeuN (C2), and combined AIF and NeuN (C3) in the non-ischemic cortex were shown respectively. AIF (C4), NeuN (C5) and combined AIF and NeuN (C6) immunohistochemistry in the ischemic cortex after permanent FCI were revealed also. AIF immunoreactivity was intensely visible in the nucleus at 4 hours after permanent FCI (arrow heads). FCI, focal cerebral ischemia; AIF, apoptosis inducing factor; NeuN, neuron-specific nuclear protein; Mito-, Mitochondrial; Ctr, control. Scale bar = 20 μm .

Table 1. Summary of the selected physiological variables of the ICR mice, measured at the time of baseline (before MCAO), ischemia (after MCAO), and before and after MnTBAP treatment. There were no statistically different parameters among the groups. Abbreviations: MCAO, middle cerebral artery occlusion; MnTBAP, manganese tetrakis (4-benzoic acid) porphyrin. n = 4~5 per each group

	ICR	MnTBAP treated ICR
	Mean value \pm SD	Mean value \pm SD
	Before MCAO	Before MnTBAP treatment
pH	7.4 \pm 0.1	7.5 \pm 0.1
PCO2(mm Hg)	29 \pm 5	28.0 \pm 2.0
PO2(mm Hg)	153.5 \pm 4.5	169 \pm 9.0
BP	83.6 \pm 6.5	79.9 \pm 7.1
Temperature()	36.8 \pm 0.3	37.1 \pm 0.7
	After MCAO	After MnTBAP treatment
pH	7.4 \pm 0.1	7.5 \pm 0.1
PCO2(mm Hg)	29.5 \pm 6.5	24.8 \pm 1.2
PO2(mm Hg)	166.3 \pm 6.4	165.2 \pm 5.8
BP	87.3 \pm 5.7	75.6 \pm 5.5
Temperature()	37.0 \pm 0.2	37.5 \pm 0.4

3 (OD: vehicle, 445.70 ± 15.10; z-VAD.fmk, 276.30 ± 13.30; MnTBAP, 287.00 ± 10.00; ANOVA, p<0.001)(Fig. 5Bb). z-VAD.fmk MnTBAP caspase-3 가 . DNA vehicle z-VAD.fmk MnTBAP (OD: vehicle, 515.00 ± 58.00; z-VAD.fmk, 399.00 ± 31.80; MnTBAP, 236.00 ± 49.00; ANOVA, p<0.001)(Fig. 5Bc). MnTBAP DNA z-VAD.fmk (P<0.001). TTC staining MnTBAP vehicle

(Fig. 5C), MnTBAP 가 . (mm³: vehicle, 92.28 ± 14.85; MnTBAP, 36.16 ± 1.21; unpaired t-test, p<0.001) caspase AIF DNA AIF 2

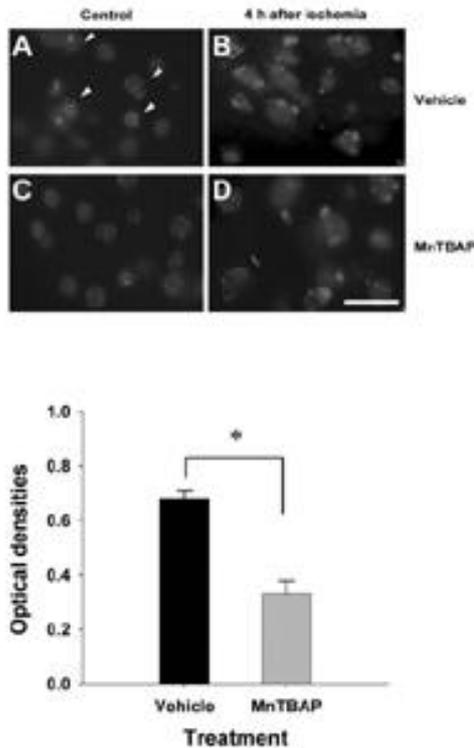


Figure 2. Representative photomicrographs showing the production of superoxide radicals by the detection of oxidized HET in both the MnTBAP- and vehicle-treated mouse brain at 4 hours after permanent FCI. Perinuclear expression of oxidized HET signals (arrow heads) is shown in the contralateral nonischemic brain (A), whereas profound increase of oxidized HET signals in the cytosol are observed in the ischemic brain of vehicle-treated mice brain (B). Expression of oxidized HET signals is barely detected in nonischemic brain (C), whereas slightly increased cytosolic expression of oxidized HET signals is observed in ischemic brain of MnTBAP-treated mice (D). MnTBAP, manganese tetrakis (4-benzoic acid) porphyrin; HET, hydroethidine. Scale bar = 20 μm.

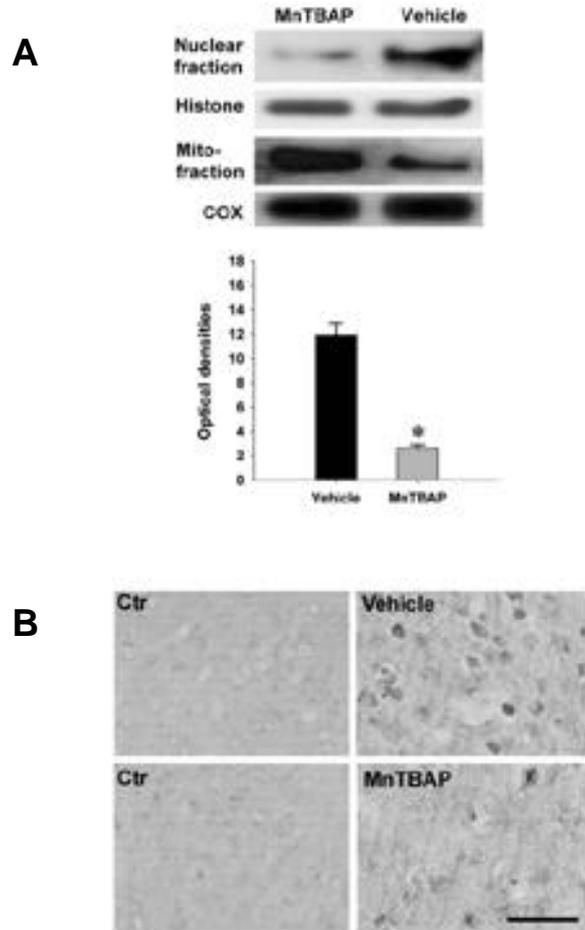


Figure 3. Inhibition of AIF translocation after MnTBAP treatment. (A) Comparisons of AIF expression between MnTBAP- and vehicle-treated mice by Western blot analysis showed decrease of AIF nuclear translocation by MnTBAP. (B) Immunohistochemistry after permanent FCI revealed significant reduction of AIF expression in MnTBAP-treated mice. Scale bar=50 μm.

가 (Fig. 1A).
 AIF NeuN (Fig. 1B, C).
 MnTBAP oxidized HEt (Fig. 2).
 MnTBAP AIF (Fig. 3).
 DNA , vehicle 24
 MnTBAP PFGE (Fig. 4).
 pan-caspase z-VAD.fmk
 AIF가 caspase
 VAD.fmk MnTBAP
 caspase

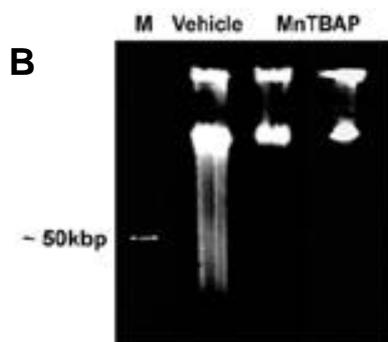
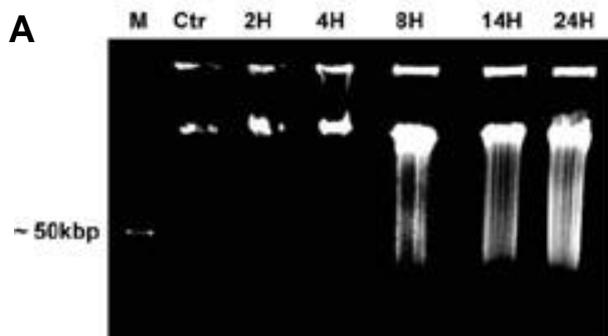


Figure 4. Representative photographic findings of large-scale DNA fragmentation using PFGE after permanent FCI and comparison between MnTBAP- and vehicle-treated mice. (A) Large-scale DNA fragmentation (mainly 50 kbp) was shown as early as 8 hours after permanent FCI. (B) The large-scale DNA fragmentation was blocked in the MnTBAP-treated mice at 24 hours after permanent FCI. PFGE, pulse field gel electrophoresis; M, marker; ctr, control.

z-VAD.fmk MnTBAP
 DNA
 MnTBAP (Fig. 5).

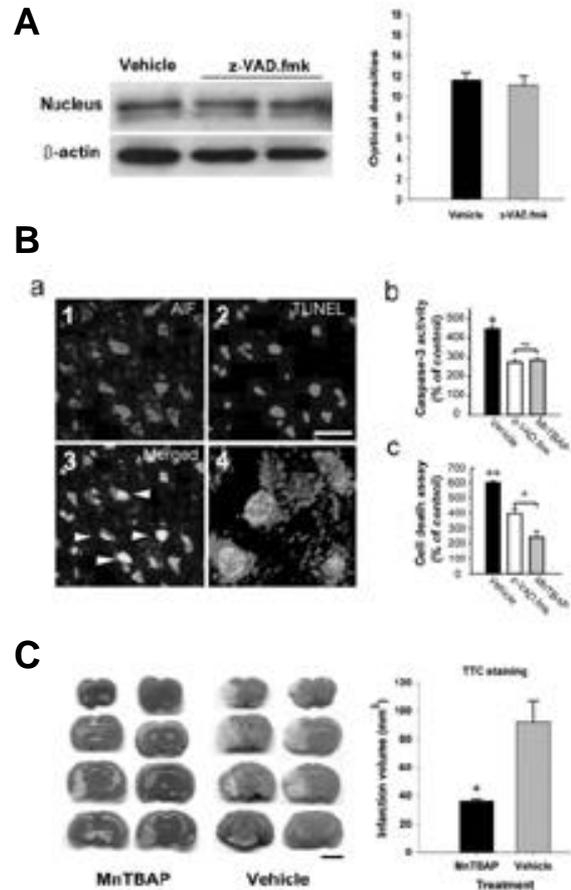


Figure 5. Western blot analysis, immunofluorescent staining, and TTC staining. (A) Nuclear translocation of AIF was not different between z-VAD.fmk- and vehicle-treated mice 4 hours after permanent FCI in Western blot analysis. (Ba) Immunofluorescent double-staining for AIF and TUNEL disclosed colocalization of AIF and TUNEL 24 hours after permanent FCI. AIF-positive cells (Ba1), TUNEL-positive cells (Ba2), combined AIF and TUNEL (Ba3), and high magnified result (Ba4). Colocalization of nuclear AIF and TUNEL-positive cells (arrow heads). Scale bar = 20 μ m. (Bb) Comparison of caspase-3 activity (*P < 0.001) and apoptosis-associated DNA fragmentation by cell death assay (Bc) 24 hours after permanent FCI among the vehicle-, z-VAD.fmk- and MnTBAP-treated mice. (C) TTC staining of vehicle- and MnTBAP-treated mice showed significant decrease of infarction volume by MnTBAP-treatment, compared with vehicle-treatment. z-VAD.fmk, N-Benzyloxycarbonyl-val-ala-asp-(O-methyl)-fluoromethyl ketone; TUNEL, terminal deoxynucleotidyl transferase-mediated uridine 5'-triphosphate biotin nick-end labeling; TTC, 2,3,5-triphenyltetrazolium chloride. Scale bar = 4 mm.

AIF가 DNA
 가 AIF
 , peroxy-nitrite [25] [27]가
 , UV
 [28] in vitro AIF
 . AIF
 , 가 가
 가 (free radical)가 mem-
 brane permeability transition (MPT)
 , MPT AIF
 [2,12,28].
 가 cytochrome c
 (proapoptotic) redox
 AIF [29].
 Bcl-2 superfamily BID BAX
 , p53
 AIF channel [15]
 herpes simplex Bcl-2 transfee
 tion , AIF
 [17]. BID BAX AIF
 [30].
 24
 TUNEL AIF [25]
 (Fig. 5Ba), [22], [19]
 AIF 가 TUNEL
 , AIF
 . z-VAD.fmk MnTBAP
 caspase-3 가
 , MnTBAP z-VAD.fmk
 가 (Fig. 5Bb-c)
 caspase
 caspase MnTBAP
 . 가
 [22,24]. AIF가 endonucle
 ase G nuclease [6,7], CAD
 가 2 AIF가
 1 [13]
 AIF가
 가 .
 MnTBAP ,
 AIF endonucle
 ase G nuclease ,

caspase nucleosomal DNA
 ,
 , cas-
 pase AIF DNA
 . MnTBAP
 가 caspase cas-
 pase
 ,
 가 .

REFERENCES

1. Chan PH. Reactive oxygen radicals in signaling and damage in the ischemic brain. *J Cereb Blood Flow Metab* 2001;21:2-14.
2. Murakami K, Kondo T, Kawase M, Li Y, Sato S, Chen SF, Chan PH. Mitochondrial susceptibility to oxidative stress exacerbates cerebral infarction that follows permanent focal cerebral ischemia in mutant mice with manganese superoxide dismutase deficiency. *J Neurosci* 1998;18:205-13.
3. Fujimura M, Morita-Fujimura Y, Kawase M, Copin JC, Calagui B, Epstein CJ, Chan PH. Manganese superoxide dismutase mediates the early release of mitochondrial cytochrome c and subsequent DNA fragmentation after permanent focal cerebral ischemia in mice. *J Neurosci* 1999;19:3414-22.
4. Kim GW, Sugawara T, Chan PH. Involvement of oxidative stress and caspase-3 in cortical infarction after photothrombotic ischemia in mice. *J Cereb Blood Flow Metab* 2000;20:1690-1701.
5. Benchoua A, Benchoua A, Guegan C, Couriaud C, Hosseini H, Sampaio N, Morin D, Onteniente B. Specific caspase pathways are activated in the two stages of cerebral infarction. *J Neurosci* 2001; 21: 7127-34.
6. Susin SA, Lorenzo HK, Zamzami N, Marzo I, Snow BE, Brothers GM, Mangion J, Jacotot E, Costantini P, Loeffler M, Larochette N, Goodlett DR, Aebersold R, SiderovskiDP, Penninger JM, Kroemer G. Molecular characterization of mitochondrial apoptosis-inducing factor. *Nature* 1999;397:441-46.
7. Arnoult D, Gaume B, Karbowski M, Sharpe JC, Cecconi F, Youle RJ. Mitochondrial release of AIF and EndoG requires caspase activation downstream of Bax/Bak-mediated permeabilization. *Embo J* 2003;22:4385-99.
8. Penninger JM, Kroemer G. Mitochondria, AIF and caspases - rivaling for cell death execution. *Nat Cell Biol* 2003;5:97-99.
9. Johnson, M. D., Kinoshita, Y., Xiang, H., Ghatan, S. & Morrison, R. S. Contribution of p53-dependent caspase

- activation to neuronal cell death declines with neuronal maturation. *J Neurosci* 1999;19: 2996-3006.
10. Lankiewicz S, Marc Luetjens C, Truc Bui N, Krohn AJ, Poppe M, Cole GM, Saïdo TC, Prehn JH. S. Activation of calpain I converts excitotoxic neuron death into a caspase-independent cell death. *J Biol Chem* 2000;275: 17064-71.
 11. Plesnila N, Zhu C, Culmsee C, Groger M, Moskowitz MA, Blomgren K. Nuclear translocation of apoptosis-inducing factor after focal cerebral ischemia. *J Cereb Blood Flow Metab* 2004;24:458-66.
 12. Daugas E, Susin SA, Zamzami N, Ferri KF, Irinopoulou T, Larochette N, Prevost MC, Leber B, Andrews D, Penninger J, Kroemer G. Mitochondrial-nuclear translocation of AIF in apoptosis and necrosis. *Faseb J* 2000;14:729-39.
 13. Susin SA, Daugas E, Ravagnan L, Samejima K, Zamzami N, Loeffler M, Costantini P, Ferri KF, Irinopoulou T, Prevost MC, Brothers G, Mak TW, Penninger J, Earnshaw WC, Kroemer G. Two distinct pathways leading to nuclear apoptosis. *J Exp Med* 2000;192:571-80.
 14. Loeffler M, Daugas E, Susin SA, Zamzami N, Metivier D, Nieminen AL, Brothers G, Penninger JM, Kroemer G. Dominant cell death induction by extramitochondrially targeted apoptosis-inducing factor. *Faseb J* 2001;15:758-67.
 15. Cregan SP, Fortin A, MacLaurin JG, Callaghan SM, Cecconi F, Yu SW, Dawson TM, Dawson VL, Park DS, Kroemer G, Slack RS. Apoptosis-inducing factor is involved in the regulation of caspase-independent neuronal cell death. *J Cell Biol* 2002;158:507-17.
 16. Ferrer I, Planas AM. Signaling of cell death and cell survival following focal cerebral ischemia: Life and death struggle in the penumbra. *J Neuropathol Exp Neurol* 2003;62:329-39.
 17. Zhao H, Yenari MA, Cheng D, Barreto-Chang OL, Sapolsky RM, Steinberg GK. Bcl-2 transfection via herpes simplex virus blocks apoptosis-inducing factor translocation after focal ischemia in the rat. *J Cereb Blood Flow Metab* 2004;24:681-92.
 18. Cao G, Clark RS, Pei W, Yin W, Zhang F, Sun FY, Graham SH, Chen J. Translocation of apoptosis-inducing factor in vulnerable neurons after transient cerebral ischemia and in neuronal cultures after oxygen-glucose deprivation. *J Cereb Blood Flow Metab* 2003;23:1137-50.
 19. Zhu C, Qiu L, Wang X, Hallin U, Cande C, Kroemer G, Hagberg H, Blomgren K. Involvement of apoptosis-inducing factor in neuronal death after hypoxia-ischemia in the neonatal rat brain. *J Neurochem* 2003;86:306-17.
 20. Klann E. Cell-permeable scavengers of superoxide prevent long-term potentiation in hippocampal area ca1. *J Neurophysiol* 1998;80:452-7.
 21. Kim GW, Noshita N, Sugawara T, Chan PH. Early decrease in DNA repair proteins, ku70 and ku86, and subsequent DNA fragmentation after transient focal cerebral ischemia in mice. *Stroke* 2001;32:1401-7.
 22. Kim GW, Kondo T, Noshita N, Chan PH. Manganese superoxide dismutase deficiency exacerbates cerebral infarction after focal cerebral ischemia/reperfusion in mice: Implications for the production and role of superoxide radicals. *Stroke* 2002;33:809-15.
 23. Saito A, Hayashi T, Okuno S, Ferrand-Drake M, Chan PH. Interaction between XIAP and Smac/DIABLO in the mouse brain after transient focal cerebral ischemia. *J Cereb Blood Flow Metab* 2003;23:1010-9.
 24. Kim GW, Lewen A, Copin J, Watson BD, Chan PH. The cytosolic antioxidant, copper/zinc superoxide dismutase, attenuates blood-brain barrier disruption and oxidative cellular injury after photothrombotic cortical ischemia in mice. *Neuroscience* 2001;105:1007-18.
 25. Zhang X, Chen J, Graham SH, Du L, Kochanek PM, Draviam R, Guo F, Nathaniel PD, Szabo C, Watkins SC, Clark RS. Intracellular localization of apoptosis-inducing factor(AIF) and large scale DNA fragmentation after traumatic brain injury in rats and in neuronal cultures exposed to peroxynitrite. *J Neurochem* 2002;82:181-91.
 26. Kim GW, Gasche Y, Grzeschik S, Copin JC, Maier CM, Chan PH. Neurodegeneration in striatum induced by the mitochondrial toxin 3-nitropropionic acid: Role of matrix metalloproteinase-9 in early blood-brain barrier disruption? *J Neurosci* 2003;23:8733-42.
 27. Fonfria E, Dare E, Benelli M, Sunol C, Ceccatelli S. Translocation of apoptosis-inducing factor in cerebellar granule cells exposed to neurotoxic agents inducing oxidative stress. *Eur J Neurosci* 2002;16:2013-6.
 28. Murahashi H, Azuma H, Zamzami N, Furuya KJ, Ikebuchi K, Yamaguchi M, Yamada Y, Sato N, Fujihara M, Kroemer G, Ikeda H. Possible contribution of apoptosis-inducing factor(AIF) and reactive oxygen species(ROS) to UVB-induced caspase-independent cell death in the T cell line Jurkat. *J Leukoc Biol* 2003;73:399-406.
 29. Kannan K, Jain SK. Oxidative stress and apoptosis. *Pathophysiology* 2000;7:153-63.
 30. Li D, Ueta E, Kimura T, Yamamoto T, Osaki T. Reactive oxygen species(ROS) control the expression of bcl-2 family proteins by regulating their phosphorylation and ubiquitination. *Cancer Sci* 2004;95:644-50.